

Early transmission dynamics of a deadly coral disease and its connection with the PortMiami Deep Dredge Project

Thomas Dobbelaere^{a,*}, other co-authors TBD, Emmanuel Hanert^{a,1}

^a*Eath and Life Institute (ELI), UCLouvain, Louvain-la-Neuve, Belgium*

Abstract

For the last 8 years, Florida's Coral Reef (FCR) has suffered from severe coral loss caused by stony coral tissue loss disease (SCTLD). The outbreak reportedly initiated near Virginia Key in September 2014, during the deepening of the Port of Miami (PoM) shipping channel, that took place between November 20, 2013 and March 16, 2015. The disease then spread to the entirety of FCR, likely through waterborne transmission. Although the causative agent of SCTLD remains unknown, there is evidence that sediments can act as vector for the disease. Here we evaluate whether sediments produced or resuspended during dredging operations could have reached reefs where the disease was first reported and assess whether the timing of these sediment fluxes was consistent with the observed spread of the disease. We evaluated the transport of sediments caused by the expansion of PoM between November 2013 and September 2014 using a quasi-3D sediment transport model forced by currents from the high-resolution coastal ocean model SLIM. A particular attention was paid to the non conventional dredging operations performed without pumping the produced chopped rock particles. Our results suggest that the dredging had close to no direct impact on the coral reefs of Virginia Key through sediment flux and sedimentation. However, a significant fraction

*Corresponding author

Email address: thomas.dobbelaere@uclouvain.be (Thomas Dobbelaere)

of the sediments produced reached monitoring sites where the disease was reported prior to September 2014, suggesting that the dredging might have played a role in the onset of the outbreak at these sites. Furthermore, using a biophysical disease agent transport model, we show that waterborne transmission from one of these sites to Virginia Key was possible before September 2014. This study brings new insight on the role that the deepening of PoM might have played in the onset of one of the worst coral outbreaks on record in the Caribbean.

Keywords: Stony coral tissue loss disease, Coastal modeling, PortMiami, Sediment plumes, Dredging

1. Introduction

2 Coral diseases are a major threat to coral reef ecosystems and have led
3 to significant declines in coral cover especially within the Caribbean region
4 (Richardson et al., 1998; Sutherland et al., 2004; Aronson and Precht, 2001;
5 Harvell et al., 2007; Brandt and McManus, 2009). One of the latest and the
6 most damaging outbreaks to date in Florida's Coral Reef (FCR) is the stony
7 coral tissue loss disease (SCTLD) (NOAA, 2018). First observed off the coasts
8 of Miami in 2014 by Precht et al. (2016), the disease has since spread through
9 the entire FCR (Muller et al., 2020; Dobbelaere et al., 2022b) and has been
10 observed in several territories of the Caribbean (Kramer et al., 2019; Meiling
11 et al., 2021; Estrada-Saldívar et al., 2021; Heres et al., 2021). Although the
12 causative agent of the disease remains unknown, the hydrodynamics is likely
13 to play an important role in its propagation as both modeling studies and ex
14 situ experiments showed evidence of waterborne disease transmission (Aeby
15 et al., 2019; Dobbelaere et al., 2020; Eaton et al., 2021; Meiling et al., 2021).
16 Furthermore, recent studies showed that sediments can act as a vector for
17 the SCTLD (Rosales et al., 2020; Studivan et al., 2022).

18 Some of the first signs of SCTLD were reported on September 26th, 2014,
19 near Virginia Key by Precht et al. (2016). In this study, a relationship was

20 derived between the time of the first outbreak at the monitored reefs and their
21 geographic distance to Virginia Key. It was therefore hypothesized that the
22 epidemic started near Virginia Key and then spread to the neighboring reefs,
23 both north and south. However, earlier signs of diseases were already reported
24 north of Virginia Key in June 2014, at the monitoring site of N. Sunny Isles
25 (Precht et al., 2016). All these observations occurred during the deepening of
26 the Port of Miami (PoM) shipping channel, that took place between November
27 20, 2013 and March 16, 2015. The dredging was monitored twice-weekly at
28 26 permanent monitoring stations established within the Miami-Dade County,
29 making it one of the most complete datasets related to a dredging project
30 (Gintert et al., 2019). Interestingly, disease signs were also reported at one of
31 these monitoring stations in May 2014 (see supplementary material Appendix
32 A).

33 While operating in a conventional way, dredged materials were pumped
34 from the dredge to a spider barge and then transported to the US Envi-
35 ronmental Protection Agency designated Ocean Dredge Material Disposal
36 Site (ODMDS) located ~8.7 km offshore. However, the suction mechanism
37 was turned off during non-conventional rock-chopping activities in order to
38 pre-treat very hard rock contained in the Anastasia and Fort Thompson
39 formations between December 2013 and May 2014 (Miller et al., 2016). U.S.
40 Army Corps of Engineers (2017) provided a back-of-the-envelope estimation
41 that this practice could have resulted in up to 33 cm deposition over 874,121
42 m² of reef surrounding the outer entrance channel . Additionally, several
43 studies reported that the impact of the dredging was widespread (Miller et al.,
44 2016), causing the death of > 560,000 corals within 0.5 km of the channel
45 (Cunning et al., 2019) and producing sediment plumes covering up to 11 km²
46 of coral area within 5-10 km of the dredging operations (Barnes et al., 2015).

47 Sediments released by dredging can affect the biological functions of
48 corals in numerous ways through turbidity and sedimentation (Erftemeijer
49 et al., 2012; Jones et al., 2015). Increased turbidity caused by the suspended

50 sediments reduces the light available to symbiotic zooxanthellae, leading to
51 reduced coral cover and growth. Sedimentation, on the other hand, can cause
52 smothering or burial of coral polyps (Erfemeijer et al., 2012; Jones et al., 2015,
53 2019). Furthermore, both sedimentation and turbidity can significantly reduce
54 larval recruitment by inhibiting settlement and reducing larval survival in the
55 water column (Jones et al., 2015). These effects are stronger with fine-grained
56 sediments, as they cause a stronger light reduction (Storlazzi et al., 2015;
57 Journey and Figueiredo, 2017). Additionally, fine-grained sediments such as
58 silts have high nutrient contents, which can lead to an increased microbial
59 activity, eventually causing anoxic conditions in the immediate vicinity of
60 corals (Weber et al., 2012). As they release finer sediments over significantly
61 longer periods than natural events such as hurricanes, dredging activities can
62 thus be more harmful to corals and reef habitat compared to other types of
63 sedimentation (Cunning et al., 2019).

64 Nonetheless, Gintert et al. (2019) argued that the reported coral mortality
65 during the dredging project was dominated by the regional outbreak of
66 SCTLD. Further, they suggested that the onset of the disease might have
67 been linked to a leaking discharge pipe of the Miami Central District Municipal
68 Wastewater Treatment Plant (WWTP) located off Virginia Key. However, as
69 sediments can act as vector for SCTLD (Studivan et al., 2022), there is also
70 a possibility that the causative agents of the disease were transported to the
71 monitoring site of Virginia Key by sediments released during the dredging.
72 This scenario can be evaluated using a sediment transport model. As coastal
73 reef ecosystems are characterized by the complex topography of the coastline
74 and the presence of islands, reefs and artificial structures, such a model
75 would require a fine spatial resolution to accurately represent the transport
76 of sediments at the reef-scale. In this context, unstructured-mesh models are
77 particularly well suited, as they can easily adapt to the topography (Fringer
78 et al., 2019) and can capture small-scale circulation features around reefs and
79 islands (Lambrechts et al., 2008).

80 The goal of this study is therefore to simulate the dispersed sediments
81 during the entirety of the PortMiami Deep Dredge Project (PMDDP) using
82 a high-resolution hydrodynamic model coupled with a sediment transport
83 model. Specifically, our goal is to answer the following questions: (1) Which
84 reefs were impacted by the PMDDP and was this impact consistent with the
85 observed timing of the onset of SCTLD ? (2) Was disease transmission to
86 Virginia Key from other diseased reefs possible before September 2014 ?

87 **2. Methods**

88 The hydrodynamics of the entire FCR was modeled using the multi-scale
89 ocean model SLIM¹, which has already been extensively validated in the
90 area (Frys et al., 2020; Dobbelaere et al., 2020, 2022a,b). SLIM uses an
91 unstructured mesh whose resolution can be locally increased in order to
92 accurately represent fine-scale flow features. The mesh used in this study
93 was built following the same methodology as Dobbelaere et al. (2020), with a
94 local refinement near PoM and in the Bay of Biscayne to achieve a resolution
95 of 100 m in the vicinity of the dredged channel (Fig. 1A). It was made up
96 of approximately 3.5×10^5 triangles and was generated with the seamsh²
97 Python library, which is based on the open-source mesh generator GMSH
98 (Geuzaine and Remacle, 2009). The model was run between October 15,
99 2013 and September 26, 2014 to cover the whole dredging period prior to the
100 observation of SCTLD on Virginia Key by Precht et al. (2016). Using such
101 a fine mesh resolution, we simulated fine-scale details of the ocean currents,
102 such as the flow acceleration between reefs and islands (Fig. 1C).

103 The transport of sediments released from dredging operations along the
104 channel was then modeled using a Lagrangian particle tracking model, forced
105 by the simulated currents. The sediment model is inspired by the Particle

¹<https://www.slim-ocean.be>

²<https://pypi.org/project/seamsh/>

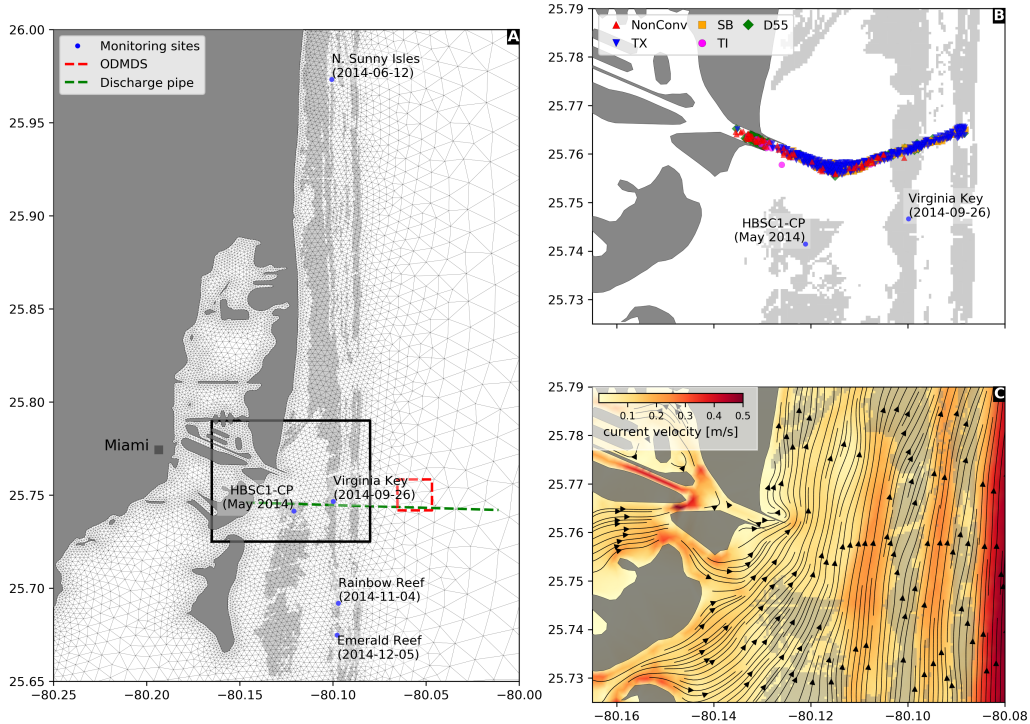


Fig. 1: **A:** Model mesh near the dredged channel. Elements have a characteristic length of 100 m over reefs (in light grey) and along the coasts (in dark gray). The monitoring sites considered in the present study are shown by blue dots. The date of the first reported signs of SCTLD at these sites is given between brackets. The Ocean Dredge Material Disposal Site (ODMDS) is shown in red and the discharge pipe of the Miami Central District Municipal Wastewater Treatment Plant in green. **B:** Close up view of the dredged channel. The locations of the different types of dredging that took place during the expansion of PortMiami are shown by colored markers. **C:** Snapshot of the modeled currents in the vicinity of the dredged channel. Small-scale flow features such as the acceleration of currents between reefs and islands are well reproduced by the model.

106 Transport Model (PTM), developed by the US Army Corps of Engineers
107 (MacDonald et al., 2006). In this model, particles undergo a combination
108 of horizontal and vertical motions. The vertical dynamics is mostly driven
109 by gravity, with heavier particles sinking faster. Once they have settled,
110 particles can be resuspended when shear stress exceeds the critical Schields
111 parameter, as parameterized by Soulsby et al. (1997). The horizontal motion
112 of the suspended particles is derived from the 2D model velocity by assuming
113 a vertical log profile, hence yielding a quasi-3D approach. When sediment
114 particles enter the near-bed zone, their horizontal velocity is greatly reduced
115 and sediments are transported with the bedload.

116 As sediment dispersion is dependent on the grain size, we modeled the
117 dispersal of five sediment classes to represent impacts of fine- to coarse-grained
118 particles: (i) 5-50 μm , (ii) 50-100 μm , (iii) 100-200 μm , (iv) 200-300 μm ,
119 and (v) 300-400 μm . We performed a different simulation for each class,
120 with the grain size randomly drawn from a uniform distribution over the
121 corresponding size range. The density of each sediment particle was derived
122 from its size using the formula of Hamilton and Bachman (1982). Furthermore,
123 all particles were differentiated based on the type of dredge that produced
124 them. Five types of dredge were considered in our modeling study (Fig. 1B):
125 (a) Texas cutterhead (TX), (b) non-conventional dredging, *i.e.* TX with
126 suction mechanism turned off (NonConv), (c) Spider Barge (SB), (d) Terrapin
127 Island hopper (TI), and (e) Dredge 55 clamshell (D55).

128 Dredging operations performed during the expansion of PoM were charac-
129 terized in our dataset by a date, a location and a type of dredge (Fig. 1B).
130 In the absence of information about the exact time of the dredging, sediment
131 particles were released from the dredging location during a whole day at a
132 rate of 80 particles/hour in the model. To account for the motion of spider
133 barges between the dredging and disposal sites, particles were released every
134 500 m along a straight line joining the dredging location to the ODMDS (see
135 Fig. 1A) for every dredging operation labelled as SB.

136 The outputs of the sediment model were then used to evaluate the tur-
137 bidity and sedimentation generated by the different dredging operations over
138 coral reefs. The occurrence of high turbidity over reefs was assessed based
139 on the concentration of suspended sediment particles in the model. This
140 concentration was computed by counting the number of suspended particles
141 inside the cells of a regular 200 m × 200 m grid over our computational
142 domain. The modeled occurrence of plume was then compared against daily
143 data of plume detection. This dataset was derived from satellite imagery by
144 Cunning et al. (2019)³ following the methods of Barnes et al. (2015) at sites
145 located within 15 km of the dredged channel. As in these two previous studies,
146 we computed the simulated plume frequency by dividing the number of days
147 during which plumes occurred by the total number of simulated days for all
148 grid cells. The impact of sedimentation was quantified by computing the
149 cumulated concentration of settled particles within the same computational
150 grid. This cumulated concentration was normalized by the total number
151 of simulated time steps to obtain an averaged concentration of deposited
152 particles over the simulated period. Higher values of this indicator would
153 indicate larger sediment deposition over a longer cumulated time.

154 The potential impact of dredging on the onset of the SLD outbreak was
155 more specifically assessed at five monitoring sites where signs of disease were
156 reported. Four sites were reefs where disease was reported in 2014 by Precht
157 et al. (2016). The fifth site was the monitoring station HBSC1-CP, used
158 throughout the expansion of PoM, where signs of disease were already reported
159 in May 2014 (Dial Cordy And Associates, 2015; Fig. 1A, see supplementary
160 material Appendix A). The impact of dredging was assessed by counting the
161 total number of sediment particles originating from each dredging that were
162 transported within 500 m of all five site. This distance was chosen to match
163 the scale of the 500 m × 500 m reef polygons used in the model (Dobbelaere

³datasets available at <https://github.com/jrcunning/pom-dredge/>

164 et al., 2020). The resulting numbers of particles were then divided by the total
165 number of sediment particles released by each type of dredging operation.
166 Larger values of this indicator would suggest a greater impact of a given type
167 of dredging operation at a given monitoring sites.

168 Finally, as previous studies showed evidence of waterborne transmission of
169 SCTLD (Aeby et al., 2019; Dobbelaere et al., 2020; Eaton et al., 2021; Meiling
170 et al., 2021), there is a possibility that the disease propagated to Virginia Key
171 from other diseased reefs affected prior to September 2014. To evaluate this
172 possibility, we computed monthly disease connectivity matrices following the
173 methodology of Dobbelaere et al. (2020) during our simulated period. These
174 connectivity matrices can be interpreted as large graphs whose vertices are 500
175 m × 500 m sub-reef polygons and whose edges represent disease connectivity
176 pathways. Evaluating the possibility of disease propagation from any sub-reef
177 A to any sub-reef B is therefore equivalent to evaluating the existence of
178 paths, *i.e.* sequences of connected vertices in the network starting from A
179 and reaching B . As computing all possible paths is not computationally
180 tractable, we limited ourselves to the computation of shortest paths from any
181 given reefs to the Virginia Key monitoring site. This was performed using the
182 function `get_all_shortest_paths` of the Python `python-igraph` package
183 (Csardi et al., 2006). Such a function requires the definition of a weight w_{ij} for
184 the edge connecting reef i to reef j . We chose $w_{ij} = 1 - \tilde{C}_{ij}$, where \tilde{C}_{ij} is the
185 probability of disease propagation from reef i to reef j , so that "shorter" edges
186 of the networks (*i.e.* connectivity pathways with smaller weights) correspond
187 to connections with larger disease propagation probability. The probability
188 of a given path was then defined as the mean connection probability of the
189 edges composing this path.

190 Finally, the 2D mode of the particle tracking model was used to assess
191 the impact of wastewater leaking from the discharge pipe mentioned by
192 Gintert et al. (2019). This model simulates the transport of neutrally buoyant
193 material driven by mean current within the water column (Dobbelaere et al.,

194 2020). Without clear information about the location of the leak, particles
195 were continuously released every 100 m along a straight line between Miami
196 Central District Municipal WWTP, located on Virginia Key and the ocean
197 discharge outfall located at 25°44'31"N 80°05'10"W (Koopman et al., 2006).
198 The impact of wastewater released from the different potential leak locations
199 was then evaluated by computing the fraction of released wastewater particles
200 that were transported within 500 m of the site of Virginia Key.

201 **3. Results**

202 Only grain sizes in the 5-50 μm range produced plumes consistent with
203 the observations of Barnes et al. (2015) and Cunning et al. (2019) (Fig. 2A).
204 For larger grain sizes, particles settled in the direct vicinity of the channel.
205 For these heavier particles, suspended sediments were only observed offshore,
206 closer to the Florida Current, where the current velocity was sufficiently
207 strong to prevent deposition. This suggests that the observed turbidity was
208 mostly due to fine silts. The modeled occurrence of plumes within 15 km
209 of the dredged matched the presence/absence data of Cunning et al. (2019)
210 in 82.7% of cases and the total area where plumes were observed was about
211 230 km^2 , consistent with the $\sim 228 \text{ km}^2$ estimated by Barnes et al. (2015).
212 Modeled plumes mostly occurred north of the dredged channel, as particles
213 were driven northward under the action of the Florida Current, with plume
214 occurring during 20% of the simulated days near the monitoring site of N.
215 Sunny Isles. Plume frequencies were lower ($\sim 5\%$) over offshore reefs but
216 reached of up to 50% over alongshore reefs. These alongshore reefs correspond
217 to regions of important sedimentation (Fig. 2B), which is consistent with the
218 correlation between plumes and sedimentation highlighted in Cunning et al.
219 (2019). The plume frequency was about 1% at site of HBSC1-CP while no
220 plume reached other southern monitoring sites during the simulation.

221 Deposition results are shown for grain sizes corresponding to silts, which are
222 more likely to carry organic matter and therefore more likely to carry SCTLD

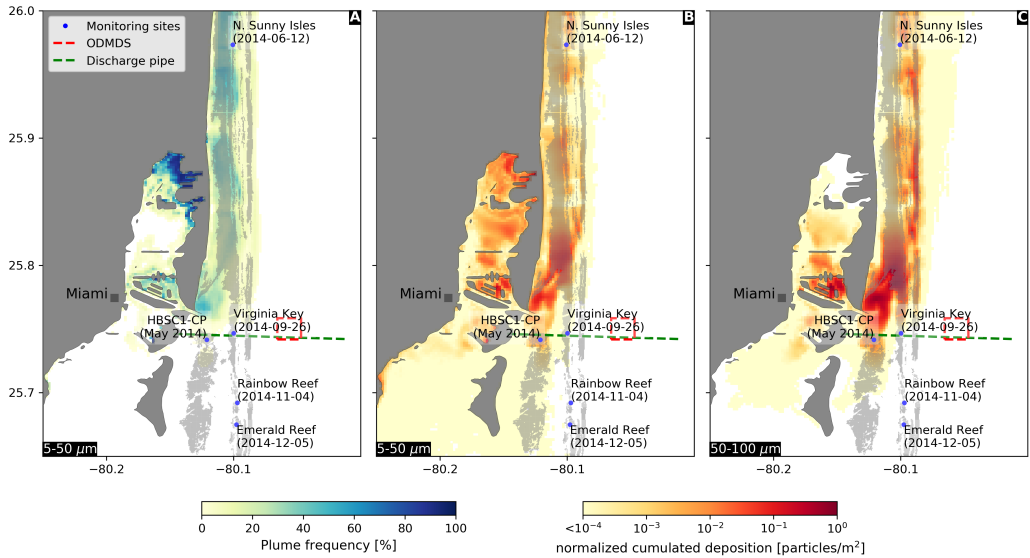


Fig. 2: **A:** Plume frequency for grain size in the range $5\text{-}50 \mu\text{m}$. The averaged concentration of deposited sediments are shown for grain sizes more likely to carry the disease: $5\text{-}50 \mu\text{m}$ (**B**) and $50\text{-}100 \mu\text{m}$ (**C**). Most modeled turbidity and sedimentation occurred north of the dredged channel. Non negligible sediment deposition occurred at site HBSC1-CP.

agents (Erfemeijer et al., 2012)(Fig. 2B,C). Sedimentation mostly occurred on reefs located north of the dredge channel. For grain sizes smaller than $5\text{-}50 \mu\text{m}$, sediments mostly settled on inshore reefs while sedimentation mostly took place on offshore reefs for grain size larger than $50\mu\text{m}$. When increasing grain sizes, the spatial distribution of sedimentation shifted southward, with a decrease of sedimentation near N. Sunny Isles and an increase of the concentration of settled sediments near HBSC1-CP and Virginia Key. The normalized cumulated deposition was around $0.01 \text{ particles/m}^2$ at site HBSC1-CP for all grain sizes while it increased from 2.5×10^{-7} to 1.6×10^{-3} with increasing grain size at Virginia Kay. For all grain sizes, no sedimentation occurred near Rainbow Reef and Emerald Reef. However, sediments settled at similar latitudes west of these sites for grain sizes below $100 \mu\text{m}$.

The evaluation of the impact of dredging at the monitoring sites indicated that dredging did not significantly impact the stations located south of the

dredged channel, except at site HBSC1-CP (Fig. 3). In contrast, up to 40% of the released sediment particles reached the northern site of N. Sunny Isles. The impact of dredging at this site decreased with increasing sediment size and the fraction of sediment particles reaching the N. Sunny Isles dropped below 2% for grain sizes larger than 200 μm . However, for grain sizes finer than 50 μm , N. Sunny Isles was heavily impacted by TX dredging. Indeed, the number of particles produced by TX reaching N. Sunny Isles was 50% larger than the cumulated number of particles produced by other dredging operations reaching the monitoring site for the same grain size. Such large impact can be explained by the fact that TX was one of the most frequent type of dredging during the simulations, with 268 simulated operations out of 734 (Fig. 3C). However, SB events occurred at an equivalent frequency but resulted in 4 times fewer particles reaching N. Sunny Isles. For grain sizes below 100 μm , between 10% and 30% of the sediments released by non conventional dredging reached N. Sunny Isles. This fraction dropped below 1% for grain sizes larger than 200 μm . The fraction of sediments produced by non conventional dredging reaching site HBSC1-CP remained between 1% and 5% for all grain sizes. For grain sizes below 100 μm , D55 and NonConv were the main sources of sediments reaching HBSC1-CP. Above 100 μm , the main source of sediments to the site became TI. The fraction of sediments produced by SB reaching HBSC1-CP remained negligible for all grain sizes. No sediment particles reached the sites of Rainbow Reef and Emerald Reef for all grain sizes. However, some particles reached Virginia Key for grain sizes larger than 100 μm . These sediments particles almost entirely originated from SB. Nonetheless, the impact of the dredging on Virginia Key remained limited with less than 1% of the released particles reaching the site.

Applying the same analysis to the discharge pipe of Miami Central District Municipal WWTP suggested that only wastewater released from a leak in the direct vicinity of the Virginia Key could have impacted the site. Fig. 4 shows the fraction of released wastewater particles that reached the site of

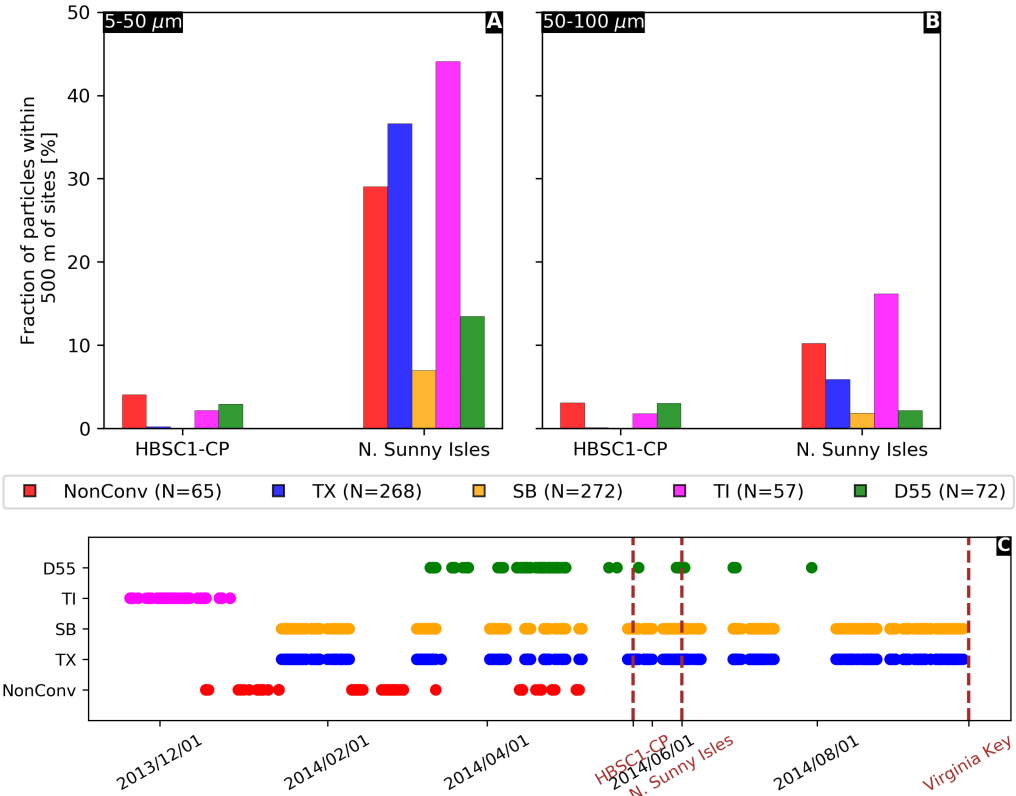


Fig. 3: Fraction of the total number of sediment particles released by each type of dredge that drifted within 500 m of HBSC1-CP and N. Sunny Isles with grain sized of 5-50 μm (**A**) and 50-100 μm (**B**). **C:** Temporal distribution of the simulated dredging operations. The dates of the first reported disease signs at each monitoring site are shown with dotted vertical lines in dark red. With the exception of HBSC1-CP, sites located south to the dredged channel were barely impacted by the dredging. However, a significant fraction of the released sediment particles reached the northern site of N. Sunny Isles. The number of simulated dredging operations is given between brackets for each dredging type

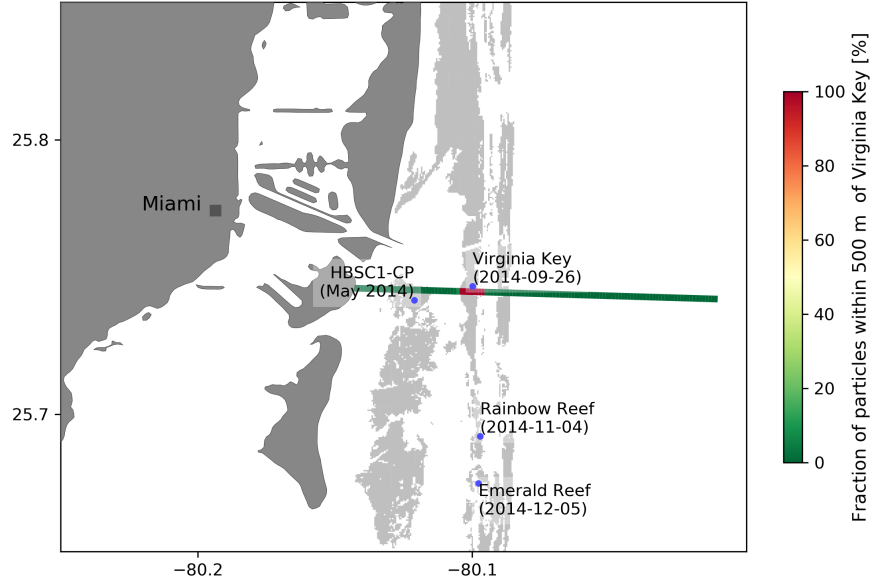


Fig. 4: Fraction of wastewater particles reaching the site of Virginia Key for potential leak positions located every 100 m along the discharge pipe. Only particles released in the direct vicinity of Virginia Key could reach the monitoring site.

267 Virginia Key for every 100 m segments of the discharge pipe. The fraction of
 268 particles that drifted within 500 m of Virginia Key was: 100% for particles
 269 released within 500 m of the site; 0-1% for particles released between 500 m
 270 and 1.5 km away from the site; and 0% for all other sources of wastewater
 271 particles. As HBSC1-CP was also located near the discharge pipe, a similar
 272 analysis was conducted for this monitoring site and gave similar results.

273 As signs of disease were observed at site HBSC1-CP in May 2014, before
 274 the first observations of SCTLD in Virginia Key in September 2014, we
 275 assessed the presence of shortest paths from HBSC1-CP to Virginia Key
 276 in the modeled monthly disease connectivity networks between May and
 277 September 2014 (Fig. 5). We found connectivity pathways connecting the
 278 two sites during all months of May-September 2014, with the exception of
 279 July. This suggests that there was a possibility of disease propagation from
 280 HBSC1-CP to Virginia Key during most of these 5 months. However, we

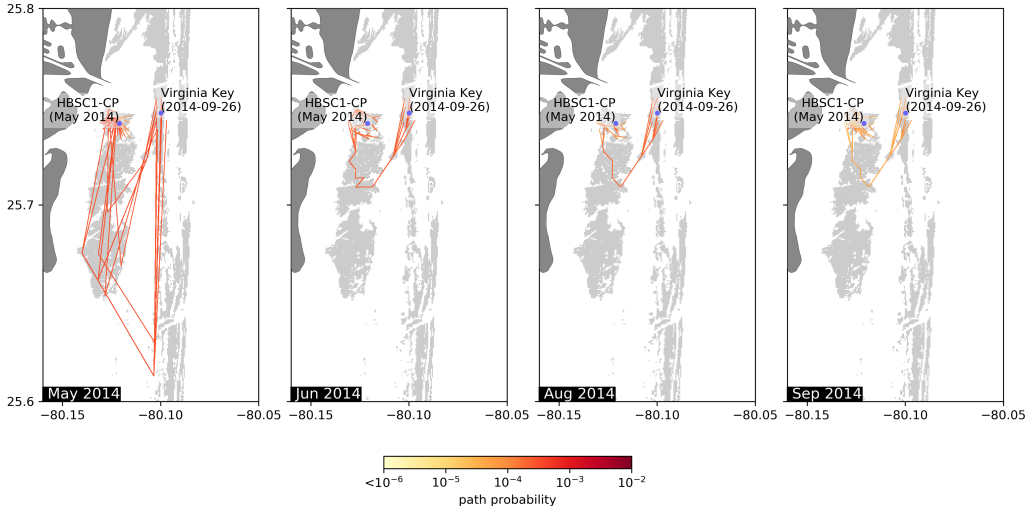


Fig. 5: Shortest path from HBSC1-CP to Virginia Key in the monthly disease connectivity networks between May and September 2014. July 2014 was the only month without modeled connectivity between the two sites between May and September 2014. Southern intermediary reefs were needed as stepping stones for the propagation of the disease from HBSC1-CP to Virginia Key.

281 found no direct pathway connecting the two sites. Southern intermediary
 282 reefs were systematically needed as stepping stones for the propagation of
 283 the disease. This suggests that several months might have been required for
 284 disease agents to reach Virginia Key from HBSC1-CP. Moreover, shortest
 285 paths in June, August and September 2014 had many sub-reef stepping stones
 286 in common. These similar connectivity patterns indicate favorable conditions
 287 for disease propagation over several months from HBSC1-CP to Virginia Key
 288 during this period.

289 4. Discussion

290 The quasi-3D sediment model forced by currents from the high-resolution
 291 coastal ocean model SLIM reproduced a sediment dynamics consistent with
 292 plume observations derived from satellite imagery. It suggests that sediment
 293 particles produced by dredging were mostly transported northward under the

294 influence of the Florida Current. No sediment particles reached the southern
295 sites of Rainbow Reef and Emerald Reef while dredging had limited direct
296 impact on Virginia Key, identified as the site where the outbreak of SCTLD
297 was initiated in September 2014 (Precht et al., 2016). Furthermore, our
298 results indicate that it is unlikely that the site was affected by a leaking
299 discharge pipe of Miami Central District Municipal WWTP, as suggested
300 by Gintert et al. (2019). However, signs of disease were observed prior to
301 September 2014 at the sites of N. Sunny Isles and HBSC1-CP, where the
302 impact of dredging was greater. Up to 30% of silt particles produced by
303 non-conventional dredging operations reached coral reefs of N. Sunny Isles
304 while 5% of them reached site HBSC1-CP, where significant sedimentation
305 occurred. Furthermore, monthly disease connectivity networks indicate that
306 disease agents could be transmitted from HBSC1-CP to the site of Virginia
307 Key.

308 Our study confirms previous reports about the widespread impact of the
309 expansion of PoM. As in Barnes et al. (2015), the total area of plumes in
310 our model was about 230 km². Furthermore, the model results reproduced
311 the plume presence/absence within 15 km of the dredged channel derived by
312 Cunning et al. (2019) with an accuracy of 82.7%. Such a good agreement
313 was only obtained for grain sizes in the range 5-50 µm, suggesting that fine
314 silts were the main drivers of the turbidity generated by dredging, which is
315 consistent with previous studies (Storlazzi et al., 2015; Fourney and Figueiredo,
316 2017). Despite this good agreement, the distribution of plumes predicted by
317 our model tends to be shifted northward compared to these previous studies.
318 These discrepancies might be explained by the fact that our approaches
319 is solely based on sediment concentration. However, turbidity depends on
320 many local factors such as the water content of phytoplankton and organic
321 matters (Gray, 2000; Thackston and Palermo, 2000). As reported by Cunning
322 et al. (2019), the plumes mostly occurred in areas of high sedimentation. As
323 such areas were mostly located over coral reefs, our results suggests that the

324 expansion of PoM might have harmed coral populations over an extended
325 area through increased turbidity and sedimentation. This sedimentation
326 mostly took place on alongshore reefs for grain sizes smaller than 50 μ m
327 and on offshore reefs for coarser grain sizes. Sediment settlement might be
328 significantly harmful to offshore coral reefs populations as they are usually
329 less accustomed to sedimentation than their inshore counterparts (Wolanski
330 et al., 2005).

331 A limitation of our study is that conventional and non-conventional dredg-
332 ing are treated in the same way in the model. For all dredging types, sediment
333 particles were released at the same rate in the model. Although conven-
334 tional dredging was reported to release fine-grained sediments in the water
335 column through dewatering and overflow from barges (Jones et al., 2016),
336 the quantity of dredged material lost in the water was limited by the use of
337 pumping mechanisms. In contrast, for non-conventional dredging, the suction
338 mechanism was turned off, causing all chopped rock particles to be released
339 in the water column. The numbers of particles reaching the monitoring sites
340 were therefore likely underestimated for non conventional dredging operations.
341 However, the fractions given in Fig. 3A,B remain valid as they are relative
342 to the total number of sediments released in the water column. The coral
343 reefs of N. Sunny Isles appeared to be highly sensitive to fine-grained sedi-
344 ments produced by dredging (Fig. 3). Furthermore, the non-conventional
345 rock-chopping that took place between December 2013 and May 2014, was
346 a non-negligible source of sediments to N. Sunny Isles, as up to 30% of the
347 released particles reached the site. As sediments have the potential to act as
348 a SCTLD vector (Rosales et al., 2020; Studivan et al., 2022), the dredging
349 might therefore have contributed to the observed onset of the disease on the
350 reefs of N. Sunny Isles in June 2014. Moreover, up to 5% of the fined-grained
351 sediments produced by non-conventional dredging reached the site HBSC1-CP
352 before May 2014, when the disease was first reported there. Although this
353 represents a more limited quantity of sediments, HBSC1 was within 2 km

354 from the sites where non-conventional dredging took place, in a region where
355 the model predicted an important sedimentation. Therefore, although fewer
356 sediments reached HBSC1-CP, they had a higher probability to settle and
357 to be in direct contact with corals. In addition to smothering corals and
358 diverting their energy through sediment removal (Erfemeijer et al., 2012),
359 these settled sediments are more likely to transmit the disease to the reefs.

360 In all simulations, the expansion of PoM had limited direct impact on
361 Virginia Key, identified as the site where the outbreak was initiated in
362 September 2014 (Precht et al., 2016). For all grain sizes, the fraction of
363 sediment particles reaching Virginia Key remained below 1%. It is therefore
364 unlikely that sediments produced by the deepening of the channel brought the
365 disease to the site. Furthermore, our simulation of leaking wastewater along
366 the discharge pipe of Miami Central District Municipal WWTP suggests
367 that currents were likely to flush wastewater away from Virginia Key. It was
368 therefore unlikely that wastewater affected the site, except if the leak was
369 located within hundreds of meters from the site. However, signs of disease
370 were observed prior to September 2014 at the sites of N. Sunny Isles and
371 HBSC1-CP, both of which were impacted by the dredging. Several studies
372 showed evidence of waterborne transmission of SCTLD (Aeby et al., 2019;
373 Dobbelaere et al., 2020; Eaton et al., 2021; Meiling et al., 2021). Disease
374 agents might therefore have been transported by currents from one of the
375 diseased sites to Virginia Key. As site HBSC-CP was the closest to Virginia
376 Key, we built and analyzed monthly disease connectivity networks and found
377 connectivity pathways from HBSC1 to Virginia Key in May, June, August
378 and September 2014. This implied that the propagation of the disease
379 from HBSC1-CP to Virginia Key through hydrodynamics-driven transport of
380 disease agents was possible during these four months. All these pathways used
381 reefs located further south as stepping stones. Therefore, the propagation of
382 SCTLD to Virginia Key starting from HBSC1-CP required these intermediary
383 reefs to be first infected by disease agents released from HBSC1-CP. Once

384 diseased, these colonies would then send disease agents to affect the next
385 colonies of the connectivity pathway until the outbreak reached Virginia Key.
386 Assuming an averaged transmission time of the order of 5-10 days (Dobbelaere
387 et al., 2020), disease propagation from HBSC1-CP to Virginia Key might
388 have required several months. This is consistent with the 5-month period
389 separating disease reports at these two sites. Moreover, the fact that June,
390 August and September exhibited similar connectivity pathways suggests that
391 disease propagation could indeed have occurred over several months without
392 being interrupted by changing hydrodynamic conditions.

393 5. Conclusion

394 In the present study, we evaluated the impact of the dredging operations
395 that took place during the deepening of the Port of Miami shipping channel on
396 the neighboring coral reefs. This evaluation was performed using a quasi-3D
397 sediment model forced by high-resolution currents from the coastal ocean
398 model SLIM. As the first signs of SCTLD were reported during the PMDDP
399 and since sediments may be a SCTLD vector, we aimed at answering two main
400 questions. First, we wanted to evaluate the fraction of sediments produced
401 by the PMDDP that reached Virginia Key and other monitoring sites where
402 the disease was reported. Second, we evaluated the possibility of waterborne
403 transmission of SCTLD to Virginia Key from other reefs impacted by the
404 dredging. Doing so, we paid a special attention to the sediments produced
405 by non conventional rock chopping during which pumping mechanisms were
406 turned off, causing all chopped rock particles to be directly released in the
407 water column.

408 Our results suggest that the dredging operations had close to no direct
409 impact on the coral reefs of Virginia Key, indicating that disease transmission
410 by sediments was extremely unlikely. However, our results show that the
411 sediments released by the non conventional dredging operations had a non-
412 negligible impact on the sites of N. Sunny Isles and HBSC1-CP, where signs

413 of disease were observed before the outbreak was first reported at Virginia
414 Key. This suggests that the sediments might have triggered the onset of the
415 disease at these two sites. Furthermore, using a previously developed bio-
416 physical model that successfully reproduced the observed spread of SCTLD,
417 we show that there was a possibility of waterborne disease propagation from
418 HBSC1-CP to Virginia Key.

419 This study suggests that the PMDDP might have played a role in the
420 onset of the outbreak of SCTLD at Virginia Key, from where the disease was
421 then reported to propagate through the entire FCR. Our work brings new
422 insight on the impact of a major dredging project in Florida on the onset of
423 one of the worst coral outbreaks on record in the Caribbean. It suggests that
424 the potential to initiate a coral disease outbreak should be taken into account
425 when considering future dredging projects.

426 Acknowledgments

427 Computational resources were provided by the Consortium des Équipements
428 de Calcul Intensif (CÉCI), funded by the F.R.S.-FNRS under Grant No.
429 2.5020.11. Thomas Dobbelaere is a PhD student supported by the Fund for
430 Research training in Industry and Agriculture (FRIA/FNRS).

431 **TODO: Some words about Jocelyn and Xaymara**

432 References

- 433 Aeby, G., Ushijima, B., Campbell, J.E., Jones, S., Williams, G., Meyer, J.L.,
434 Hase, C., Paul, V., 2019. Pathogenesis of a tissue loss disease affecting
435 multiple species of corals along the Florida Reef Tract. *Frontiers in Marine
436 Science* 6, 678.
- 437 Aronson, R.B., Precht, W.F., 2001. White-band disease and the changing face
438 of Caribbean coral reefs, in: *The ecology and etiology of newly emerging
439 marine diseases*. Springer, pp. 25–38.

- 440 Barnes, B.B., Hu, C., Kovach, C., Silverstein, R.N., 2015. Sediment plumes
441 induced by the Port of Miami dredging: Analysis and interpretation using
442 Landsat and MODIS data. *Remote Sensing of Environment* 170, 328–339.
- 443 Brandt, M.E., McManus, J.W., 2009. Dynamics and impact of the coral
444 disease white plague: insights from a simulation model. *Diseases of aquatic
445 organisms* 87, 117–133.
- 446 Csardi, G., Nepusz, T., et al., 2006. The igraph software package for complex
447 network research. *InterJournal, complex systems* 1695, 1–9.
- 448 Cunning, R., Silverstein, R.N., Barnes, B.B., Baker, A.C., 2019. Extensive
449 coral mortality and critical habitat loss following dredging and their associa-
450 tion with remotely-sensed sediment plumes. *Marine pollution bulletin*
451 145, 185–199.
- 452 Dial Cordy And Associates, 2015. Quantitative Post-construction Analysis
453 for Hardbottom Benthic Communities, Miami Harbor Phase III Federal
454 Channel Expansion Project Permit No. 0305721-001-BI.
- 455 Dobbelaere, T., Curcic, M., Le Hénaff, M., Hanert, E., 2022a. Impacts of
456 Hurricane Irma (2017) on wave-induced ocean transport processes. *Ocean
457 Modelling* , 101947doi:10.1016/j.ocemod.2022.101947.
- 458 Dobbelaere, T., Holstein, D.M., Muller, E.M., Gramer, L.J., McEachron, L.,
459 Williams, S.D., Hanert, E., 2022b. Connecting the dots: Transmission of
460 stony coral tissue loss disease from the Marquesas to the Dry Tortugas.
461 *Frontiers in Marine Science* doi:10.3389/fmars.2022.778938.
- 462 Dobbelaere, T., Muller, E.M., Gramer, L.J., Holstein, D.M., Hanert, E., 2020.
463 Coupled epidemiological-hydrodynamic modeling to understand the spread of a
464 deadly coral disease in Florida. *Frontiers in Marine Science* 7, 1016.
- 465 Eaton, K.R., Landsberg, J.H., Kiryu, Y., Peters, E.C., Muller, E.M., 2021.
466 Measuring stony coral tissue loss disease induction and lesion progression

- 467 within two intermediately susceptible species, Montastraea cavernosa and
468 Orbicella faveolata. *Frontiers in Marine Science* , 1287.
- 469 Erftemeijer, P.L., Riegl, B., Hoeksema, B.W., Todd, P.A., 2012. Environmental
470 impacts of dredging and other sediment disturbances on corals: a
471 review. *Marine pollution bulletin* 64, 1737–1765.
- 472 Estrada-Saldívar, N., Quiroga-García, B.A., Pérez-Cervantes, E., Rivera-
473 Garibay, O.O., Alvarez-Filip, L., 2021. Effects of the Stony Coral Tissue
474 Loss Disease outbreak on coral communities and the benthic composition
475 of Cozumel reefs. *Frontiers in Marine Science* 8, 306.
- 476 Fourney, F., Figueiredo, J., 2017. Additive negative effects of anthropogenic
477 sedimentation and warming on the survival of coral recruits. *Scientific
478 reports* 7, 1–8.
- 479 Fringer, O.B., Dawson, C.N., He, R., Ralston, D.K., Zhang, Y.J., 2019. The
480 future of coastal and estuarine modeling: Findings from a workshop. *Ocean
481 Modelling* 143, 101458.
- 482 Frys, C., Saint-Amand, A., Le Hénaff, M., Figueiredo, J., Kuba, A., Walker,
483 B., Lambrechts, J., Vallaeyns, V., Vincent, D., Hanert, E., 2020. Fine-scale
484 coral connectivity pathways in the Florida Reef Tract: Implications for
485 conservation and restoration. *Frontiers in Marine Science* 7, 312.
- 486 Geuzaine, C., Remacle, J.F., 2009. Gmsh: A 3-D finite element mesh generator
487 with built-in pre-and post-processing facilities. *International journal for
488 numerical methods in engineering* 79, 1309–1331.
- 489 Gintert, B.E., Precht, W.F., Fura, R., Rogers, K., Rice, M., Precht, L.L.,
490 D'Alessandro, M., Croop, J., Vilmar, C., Robbart, M.L., 2019. Regional
491 coral disease outbreak overwhelms impacts from a local dredge project.
492 *Environmental monitoring and assessment* 191, 1–39.

- 493 Gray, J.R., 2000. Comparability of suspended-sediment concentration and
494 total suspended solids data. 4191, US Department of the interior, US
495 Geological Survey.
- 496 Hamilton, E.L., Bachman, R.T., 1982. Sound velocity and related properties
497 of marine sediments. *The Journal of the Acoustical Society of America* 72,
498 1891–1904.
- 499 Harvell, D., Jordán-Dahlgren, E., Merkel, S., Rosenberg, E., Raymundo, L.,
500 Smith, G., Weil, E., Willis, B., 2007. Coral disease, environmental drivers,
501 and the balance between coral and microbial associates. *Oceanography* 20,
502 172–195.
- 503 Heres, M.M., Farmer, B.H., Elmer, F., Hertler, H., 2021. Ecological conse-
504 quences of stony coral tissue loss disease in the Turks and Caicos Islands.
505 *Coral Reefs* 40, 609–624.
- 506 Jones, R., Bessell-Browne, P., Fisher, R., Klonowski, W., Slivkoff, M., 2016.
507 Assessing the impacts of sediments from dredging on corals. *Marine Pollu-
508 tion Bulletin* 102, 9–29.
- 509 Jones, R., Fisher, R., Bessell-Browne, P., 2019. Sediment deposition and coral
510 smothering. *PLoS One* 14, e0216248.
- 511 Jones, R., Ricardo, G., Negri, A., 2015. Effects of sediments on the reproduc-
512 tive cycle of corals. *Marine Pollution Bulletin* 100, 13–33.
- 513 Koopman, B., Heaney, J.P., Cakir, F.Y., Rembold, M., Indeglia, P., Kini,
514 G., 2006. Ocean outfall study. Florida Department of Environmental
515 Protection, Tallahassee .
- 516 Kramer, P., Roth, L., Lang, J., 2019. Map of stony coral tissue loss disease
517 outbreak in the Caribbean. URL: www.agrra.org. ArcGis Online. (accessed
518 June 12, 2020).

- 519 Lambrechts, J., Hanert, E., Deleersnijder, E., Bernard, P.E., Legat, V.,
520 Remacle, J.F., Wolanski, E., 2008. A multi-scale model of the hydrodynamics
521 of the whole Great Barrier Reef. *Estuarine, Coastal and Shelf Science*
522 79, 143–151.
- 523 MacDonald, N.J., Davies, M.H., Zundel, A.K., Howlett, J.D., Demirbilek,
524 Z., Gailani, J.Z., Lackey, T.C., Smith, J., 2006. PTM: particle tracking
525 model. Report 1: Model theory, implementation, and example applications.
526 Technical Report. Engineer Research And Development Center Vicksburg
527 MS Coastal And Hydraulics Lab.
- 528 Meiling, S.S., Muller, E.M., Lasseigne, D., Rossin, A., Veglia, A.J., MacKnight,
529 N., Dimos, B., Huntley, N., Correa, A., Smith, T.B., et al., 2021. Variable
530 species responses to experimental stony coral tissue loss disease (SCTLD)
531 exposure. *Frontiers in Marine Science* 8, 464.
- 532 Miller, M.W., Karazsia, J., Groves, C.E., Griffin, S., Moore, T., Wilber, P.,
533 Gregg, K., 2016. Detecting sedimentation impacts to coral reefs resulting
534 from dredging the Port of Miami, Florida USA. *PeerJ* 4, e2711.
- 535 Muller, E.M., Sartor, C., Alcaraz, N.I., van Woesik, R., 2020. Spatial
536 epidemiology of the Stony-Coral-Tissue-Loss Disease in Florida. *Frontiers*
537 in Marine Science
- 538 NOAA, 2018. Stony Coral Tissue Loss Disease
539 Case Definition. URL: <https://nmsfloridakeys.blob.core.windows.net/floridakeys-prod/media/docs/20181002-stony-coral-tissue-loss-disease-case-definition.pdf>.
540 Accesssed on June 4, 2020.
- 541 Precht, W.F., Gintert, B.E., Robbart, M.L., Fura, R., Van Woesik, R., 2016.
542 Unprecedented disease-related coral mortality in Southeastern Florida.
543 Scientific Reports 6, 1–11.

- 546 Richardson, L.L., Goldberg, W.M., Carlton, R.G., Halas, J.C., 1998. Coral
547 disease outbreak in the Florida Keys: plague type II. *Revista de Biología*
548 *tropical* , 187–198.
- 549 Rosales, S.M., Clark, A.S., Huebner, L.K., Ruzicka, R.R., Muller, E., 2020.
550 Rhodobacterales and Rhizobiales are associated with stony coral tissue loss
551 disease and its suspected sources of transmission. *Frontiers in Microbiology*
552 11, 681.
- 553 Soulsby, R., Whitehouse, R., et al., 1997. Threshold of sediment motion in
554 coastal environments, in: *Pacific Coasts and Ports'97*. Proceedings, pp.
555 149–154.
- 556 Storlazzi, C.D., Norris, B.K., Rosenberger, K.J., 2015. The influence of
557 grain size, grain color, and suspended-sediment concentration on light
558 attenuation: Why fine-grained terrestrial sediment is bad for coral reef
559 ecosystems. *Coral Reefs* 34, 967–975.
- 560 Studivan, M.S., Rossin, A.M., Rubin, E., Soderberg, N., Holstein, D.M.,
561 Enochs, I.C., 2022. Reef sediments can act as a stony coral tissue loss
562 disease vector. *Frontiers in Marine Science* , 2046.
- 563 Sutherland, K.P., Porter, J.W., Torres, C., 2004. Disease and immunity in
564 Caribbean and Indo-Pacific zooxanthellate corals. *Marine Ecology Progress Series*
565 266, 273–302.
- 566 Thackston, E., Palermo, M.R., 2000. Improved methods for correlating
567 turbidity and suspended solids for monitoring. US Army Engineer Research
568 and Development Center.
- 569 U.S. Army Corps of Engineers, 2017. Water and Air Research,
570 Inc. 2017. Contract W912EP-15-A-0002-0003 Final Miami Task 1
571 Report. URL: <https://usace.contentdm.oclc.org/utils/getfile/collection/p16021coll7/id/11844>. Accessed on February 8, 2022.

- 573 Weber, M., De Beer, D., Lott, C., Polerecky, L., Kohls, K., Abed, R.M.,
574 Ferdelman, T.G., Fabricius, K.E., 2012. Mechanisms of damage to corals
575 exposed to sedimentation. *Proceedings of the National Academy of Sciences*
576 109, E1558–E1567.
- 577 Wolanski, E., Fabricius, K., Spagnol, S., Brinkman, R., 2005. Fine sediment
578 budget on an inner-shelf coral-fringed island, Great Barrier Reef of Australia.
579 *Estuarine, Coastal and Shelf Science* 65, 153–158.

580 Appendix A. Reported disease signs at site HBSC1-CP in May
581 2014

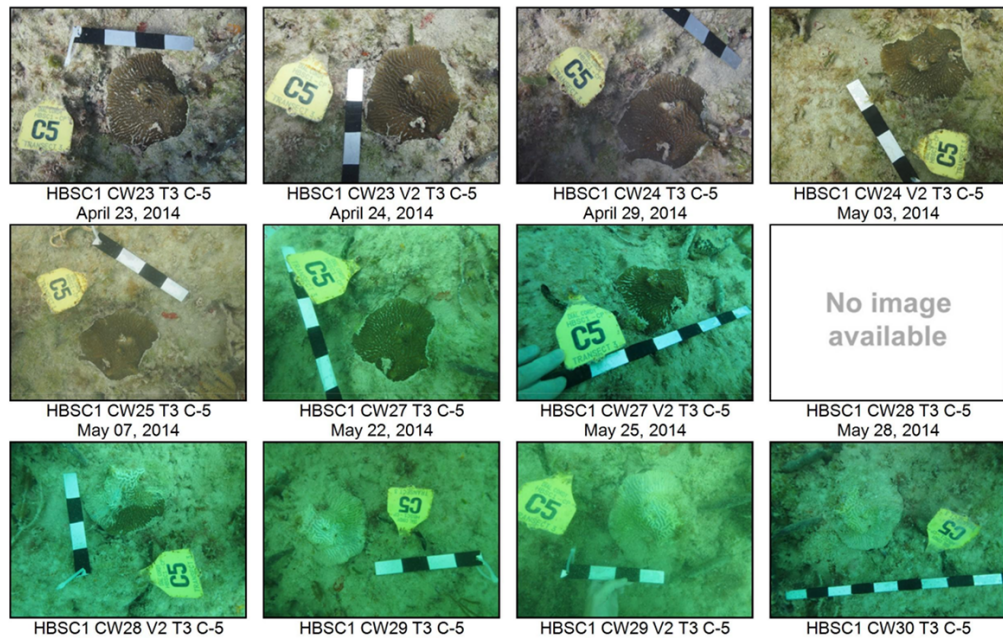


Fig. A.6: Pictures of a monitored colony at site HBSC1-CP (Dial Cordy And Associates, 2015). The first signs of the disease appeared between May 25 and May 30. By June 4, the whole colony was completely dead